Nov 7th, 12:00 AM - Nov 8th, 12:00 AM

On the Effect of Web Stiffening of Cold-Formed Steel Thin-Walled Lipped Sigma Sections in Compression Members

Rashideddin Cheraghi

Hamidreza Mohammadzadeh

Wei-Wen Yu International Specialty Conference on Cold-Formed Steel Structures
St. Louis, Missouri, U.S.A., November 7 & 8, 2018

On the effect of web stiffening of cold-formed steel thin-walled lipped sigma sections in compression members

Rashideddin Cheraghi[1] and Hamidreza Mohammadzadeh[2]

Abstract

Cold-formed steel cross sections are high strength thin-walled profiles which are highly prone to local and distortional instabilities. Stiffening techniques are utilized in the industry as a solution to enhance local and distortional buckling strengths. The sigma section is that channel section which its web pushed inward for the stiffening reason. In this research, the effect of side sway of the web (d_x) on the buckling behavior of lipped sigma sections is investigated. The results demonstrate that stiffening inclined components of the web in lipped sigma sections for d_x up to 0.5512”(14 mm) act as a stiffener and change the dominant mode of the cross section from the local buckling for the non-stiffened web to the distortional buckling for the stiffened web, and as this value rises, more reduction in the formation of local buckling in the web can be observed, but for the amount more than 0.5512”(14 mm), these components of the web act as an independent element and constrain the vertical parts of the web and local buckling of sub-elements of the web is the dominant mode. Also under a parametric study, the effect of d_x on the Euler-local and distortional buckling strengths and influential parameters on them is investigated and the d_x value for an optimum design is computed. Outcomes demonstrate that the more rise in the amount of d_x augments the Euler-local and distortional buckling strengths and the optimum value of d_x is 0.3937”(10 mm) for the target lipped sigma section.

[1]Technical Office Manager, PanahSazAlvand Eng. Co.
PhD Student, Khajeh Nasir Toosi University of Technology, Tehran, Iran
[2]CEO, Aria TadbirPazh Eng. Co.
PhD Student, Islamic Azad University-South Tehran Branch, Tehran, Iran

Introduction

High-strength cold-formed steel sections are commonly used in a variety of applications including residential construction. These steel sections typically have a nominal yield stress of 80 ksi (550 MPa) and the use of such high-strength material allows for a reduction in thickness(Yap and Hancock 2011).

Application of high-strength cold-formed steel sections with a very thin wall may lead to an optimum design but the reduction in thickness makes the cross section prone to the severe local buckling. In the industry, in order to prevent local buckling, manufacturers make complex shapes including stiffeners by folding of the elements of the cross section. However, even these complex shapes exhibit structural instabilities such local, distortional, and flexural-torsional buckling modes, and in some cases, interaction of the local and distortional buckling modes may occur (Yang and Hancock 2004; Yap and Hancock 2008, 2011).

One of the complex cross-sections reinforced with web stiffeners, considered as an innovative cross-section in the cold-formed steel industry(Schafer 2011) and demonstrated higher buckling strength rather than other counterparts (Wang et al. 2016) is the lipped sigma section. The configuration of this cross-section is illustrated in Fig. 1. The difference of lipped sigma section with lipped C section is that its web is divided into 3 sub-elements and 2 inclined components connect these sub-elements together.

Fig. 1 The shape of a lipped sigma section

In a research done by (Wang et al. 2016), it was illustrated that for lipped sigma sections, where the length of these sub-elements of the web are identical, the

lipped sigma sections demonstrate the best load bearing capacity under compression.

In this research, the amount of side sway of the web, on the buckling **behavior** and buckling **strengths** of a thin-walled lipped sigma section under compression is investigated and the results are compared with the lipped C section. To investigate the buckling behavior of the lipped sigma section, the finite strip method (FSM) and constraint finite strip method (c-FSM) are utilized (CUFSM 2006; Schafer and Ádány 2006). The results demonstrate that the increment of d_x, the horizontal projection of inclined elements' length, or, i.e. side sway of the web, significantly influences the buckling modes, the critical unbraced buckled length and the load factor (p_{cr}/p_y).

Also under a parametric study, the effect of d_x on the Euler-local buckling strength, distortional buckling strength and the influential parameters on them is investigated. The results demonstrate that the increase of d_x, augments the both the Euler-local and distortional buckling strengths. Also the value of d_x for an optimum design is computed. Design of the cross-sections are conducted based on the North American Specification AISI S100-16. (*AISI S100-16, North American Specification for the Design of Cold-Formed Steel Structural Members* 2016, *AISI S100-16, North American Specification for the Design of Cold-Formed Steel Structural Members, Commentary*)

The Case Studies

As illustrated in Fig. 2, the lipped C section of C5.5-1.63-0.75-0.0236/inch (C139.7-41.4-19.05-0.6/mm) and the lipped sigma section of Σ5.5-1.63-0.75-0.0236/inch are selected as the case studies. The web stiffeners are thin inclined components including two important features, d_x and d_y. d_x is the horizontal projection of the web stiffeners' length (i.e. the amount of side sway of web) and is the main variable in this study. d_y is the vertical projection of the web stiffeners' length assumed constant and equal to 0.15748"(4 mm) in this study. The 3 sub-elements of the web are assumed to have identical length. In Fig. 2, the dimensional parameters of the case studies are illustrated.
(C/Σ W-B-D-t)
The case studies all are compression members with the height of 9.8425' (3 meters) which is constrained with bridges at level 3.281'(1 m) and level 6.562'(2 m).

The Calculation of section properties

To simplify parametric study, section properties calculations are conducted by an assumption. It is assumed that the bent corners of lipped C and sigma sections as perpendicular corners and middle lines of $\bar{a}$, $\bar{b}$ and $\bar{c}$ are utilized in the calculation. However the amount of error is evaluated rather than exact values. As depicted in Table 1, the error of this assumption is less than 6%.

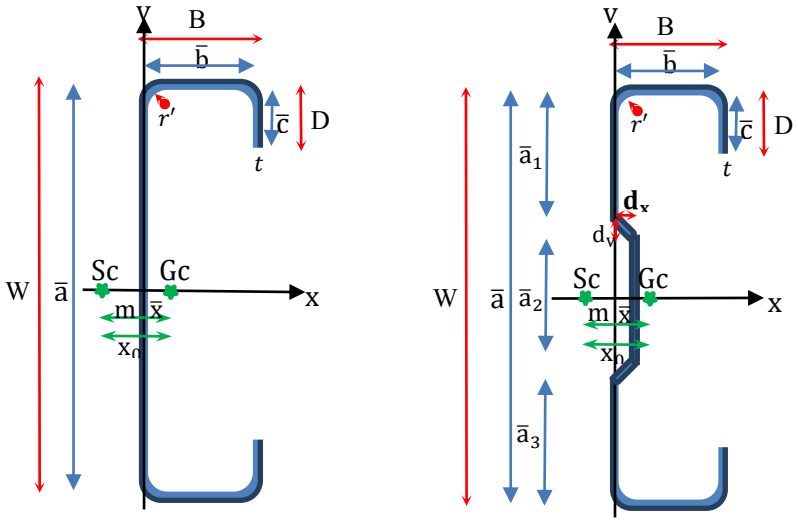

a) A Lipped C Section b) A Lipped Σ Section

Fig. 2 Dimensional characteristics of the target sections

Table 1 Comparison of section properties between approximate section and exact section of the lipped C section of C5.5-1.63-0.75-0.0236/inch

Lipped C-Section 140-40-19-1.5	APPROXIM	EXACT-CUFSM	Error(%)
A inch^2(mm^2)	0.590(381.9)	0.574(371.9)	2.70
$I_x$inch^4(mm^4)	2.644(1100349.4)	2.527(1051822.9)	4.61
I_y inch^4(mm^4)	0.231(96080.7)	0.219(91075.2)	5.50
$\bar{X}$ inch(mm)	0.472(12.0)	0.463(11.8)	1.89
m inch (mm)	-0.773(-19.6)	-0.769(-19.5)	0.53
x_0 inch (mm)	-1.245(-31.6)	-1.233(-31.3)	1.04
J inch^4 (mm^4)	0.00069(286.4)	0.00067(278.9)	2.70
C_ω inch^6 (mm^6)	1.55(416215251.3)	1.463(392843326.4)	5.95

Material Properties

The mechanical properties of the applied cold-formed steel are presented in Table 2.

Table 2 Mechanical Material Properties of applied Cold-formed steel

Mechanical Material Properties of Applied Cold-formed Steel			
Modulus of Elasticity	E	29007.5 (200000)	Ksi (Mpa)
Shear Modulus	G	11156.7(76923)	Ksi (Mpa)
Poisson Ratio	ν	0.3	-
Yield Tensile Strength	F_y	43.5(300)	Ksi (Mpa)
Ultimate Tensile Strength	F_u	50 (345)	Ksi (Mpa)

Results and Discussion

1. Buckling behavior of case studies

To investigate the buckling mode shapes of the case studies, the FSM and c-FSM are utilized. As depicted in Fig. 3, in the section with d_x=0, the simple web section, in the critical compression load, the local buckling of the web is the critical buckled shape which is occurred in the unbraced length of 3.937”(100 mm). For the section with d_x=0.07874” (2 mm), the first sigma section, in the critical compression load, the critical buckled mode shape is distortional which is occurred in the unbraced length of 35.433”(900 mm). It is also evident from the comparison of aforementioned case studies that load factor (p_{cr}/p_y) increased from 0.066 to 0.288 which is a considerable augmentation. As a check point, the participation of each buckling mode (G=global, D=distortional, L=local) in the critical load is illustrated below each case study.

The next 2 case studies are those with d_x=0.3937”(10 mm) and d_x=0.4724”(12 mm). In Fig. 3, the buckled mode shapes for these case studies were illustrated, but because of the constrained boundary conditions of the case studies, the illustrated buckled shapes in Fig. 3 are not valid, so the modified buckled shapes of these case studies are illustrated in Fig. 4. As illustrated in Fig. 4, the governing buckled shapes of the sections are still distortional, more

augmentation in the load factors is evident and just a change in the unbraced length for the case study with d_x=0.4724”(12 mm) is evident.

The last case studies are those with d_x=0.5512”(14 mm)and d_x=0.7874”(20 mm). As illustrated in Fig. 3, from d_x=0.5512”(14 mm) to the next, the buckled mode shapes change. The inclined elements of the web, constrain the movement of the web and local buckling of each part of the web is evident. The unbraced length for the both following cases are 50 mm and the load factors (p_{cr}/p_y) of the both are about 0.481.

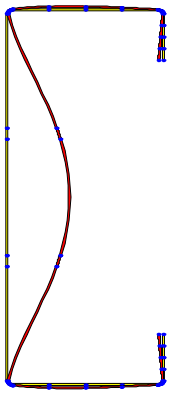			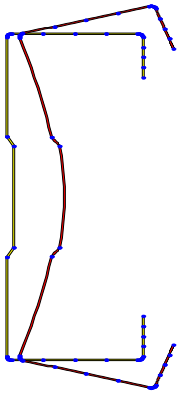		
d_x=0	L=3.9370” (100mm)	Load Factor=0.066	**d_x=0.07874” (2mm)**	L=35.433” (900mm)	Load Factor=0.288
G=0.2%	D=43.7%	L=56.1%	G=10.1%	D=89.2%	L=0.7%
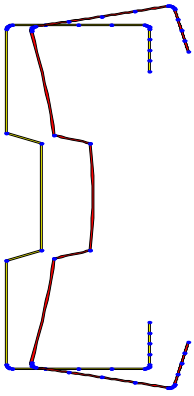			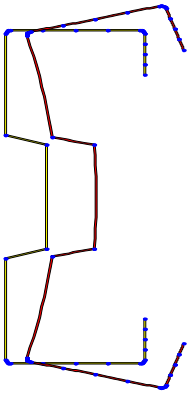		
d_x=0.39370” (10mm)	L=59.055” (1500mm)	Load Factor=0.304	**d_x=0.47244” (12mm)**	L=59.055” (1500mm)	Load Factor=0.220

G=39.5%	D=60.2%	L=0.3%	G=28%	D=71.8%	L=0.2%
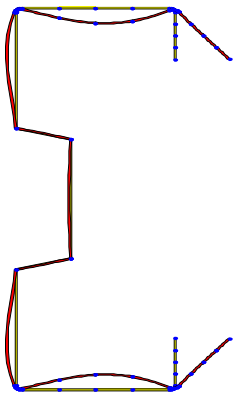			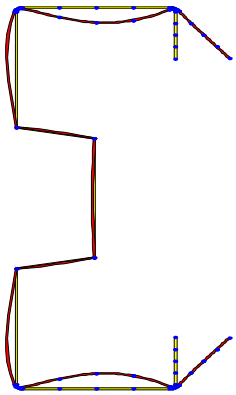		
d_x=0.55118" (14mm)	L=1.9685" (50mm)	Load Factor=0.482	**d_x=0.78740" (20mm)**	L=1.9685" (50mm)	Load Factor=0.481
G=0.1%	D=88.2%	L=11.5%	G=0.1%	D=88.4%	L=11.4%

Fig. 3 Buckled mode shape of the case studies in the critical buckling load

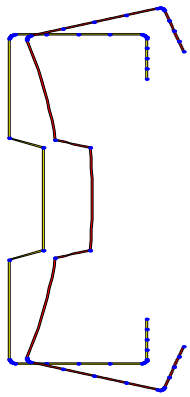			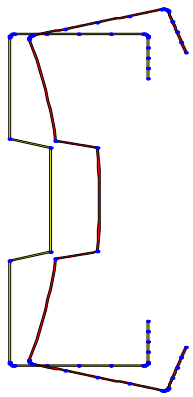		
d_x=0.39370" (10mm)	L=35.433" (900mm)	Load Factor=0.417	**d_x=0.47244" (12mm)**	L=39.370" (1000mm)	Load Factor=0.442
G=16.8%	D=82.8%	L=0.4%	G=23.1%	D=76.5%	L=0.3%

Fig. 4 Modified buckled mode shape of the case studies with d_x=10mm and d_x=12mm based on the restraining boundary conditions

2. Effect of d_x on Compression Strengths

In this section, the effect of d_x on the Euler-local buckling strength (P_n), distortional buckling strength (P_{nd}) and the influential parameters on them is investigated. The parameters includes effective web ratio, effective area ratio, polar radius of gyration of cross section (r_0), warping constant (C_ω), radius of gyration of cross-section about Y centroidal principal axis (r_y), Euler buckling stress (F_n) and distortional buckling stress (F_{nd}).

Effective web ratio= effective width of the web/ gross width of the web	$\Sigma b_{ew}/\Sigma b_w$
Effective Area ratio= effective Area / gross Area of the cross-section	A_e/A_g

2.1. Effect of d_x on Effective Web ratio and Effective Area Ratio

Effective web ratio is defined as an index to demonstrate the ratio of effectiveness of the web. As illustrated in Fig. 5, the increment of effective web ratio is proportional to the increase of d_x and this ratio is equal to 0.24 for d_x=0 and 0.67 for d_x=0.3937”(10 mm). In the region of $0 \leq d_x \leq 0.3937$”(10 mm), the slope of the curve is steep, but after this region till d_x=0.07874”(12 mm), the slope becomes negative and after this point the slope is almost zero. By the investigation of k_{loc} (Plate buckling coefficient for local sub-element buckling) and k_d (Plate buckling coefficient for distortional buckling) values for the web of the case studies based on Eq. 1.4.1.1-1 and Eq. 1.4.1.1-2 of the Appendix 1 of the AISI S100-16, respectively, prior to d_x=0.5512”(14 mm), k_d has lower value than k_{loc}, so distortional buckling is the governing mode for the web. Around d_x=0.5512”(14 mm), $k_{loc}=k_d$. From $d_x \geq 0.5512$”(14 mm), k_{loc} has lower value than k_d, so the local buckling of sub-element is governing mode. These results are in consistency with the outcomes of elastic buckling analyses done on the case studies in the preceding section. As aforementioned results indicate, from $d_x \geq 0.5512$”(14 mm), inclined elements of the web act as independent elements and not as stiffening components. Therefore, the provisions of section 1.4 of Appendix 1 of AISI S100-16 for the calculation of effective width of the stiffening elements are not valid and as a consequence, the provisions of section 1.1 of Appendix 1 of AISI S100-16 should be applied for each inclined element. By above explanations, the results demonstrated for effective web ratio for $d_x \geq 0.5512$”(14 mm) in Fig. 5 are not valid. The modified values are illustrated in Fig. 6. After the correct calculation of the effective width of the web for different values of d_x, effective area of the case studies can be computed. In Fig. 7, the effective area ratio vs. d_x is depicted.

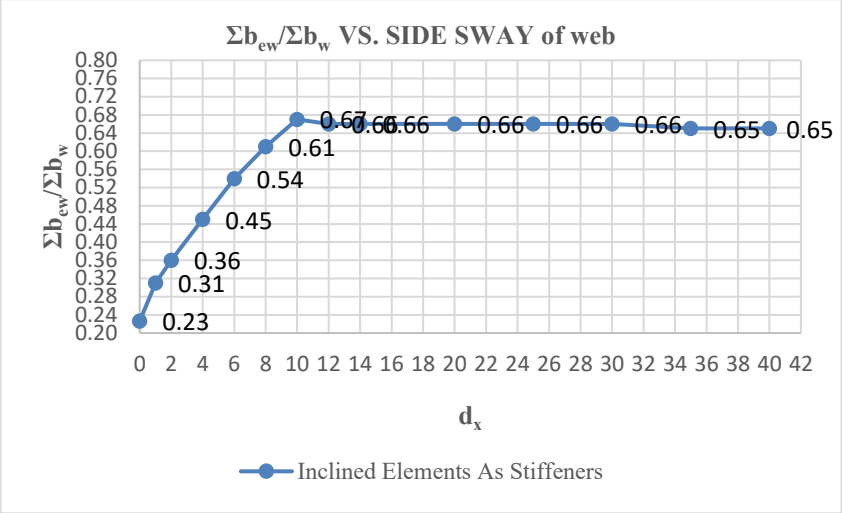

Fig. 5 The effect of d_x on effective web ratio

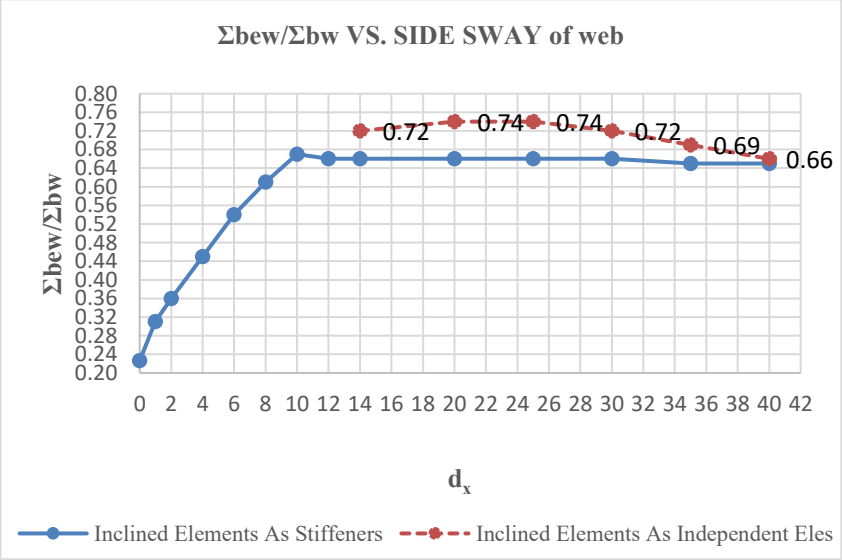

Fig. 6 The effect of d_x on modified effective web ratio

In Fig. 7, the maximum effective area ratio is 69% in the region of 0.7874”(20 mm)≤d_x≤0.9449”(24 mm). However this d_x, because of high consumption of cold-formed steel is not an economical side sway. In d_x=0.3937”(10 mm), the effective area ratio is 65% which is not far away maximum value of 69%. Therefore, this side sway may be an optimum one; less consumption of the cold-formed steel and high effectiveness of the cross section.

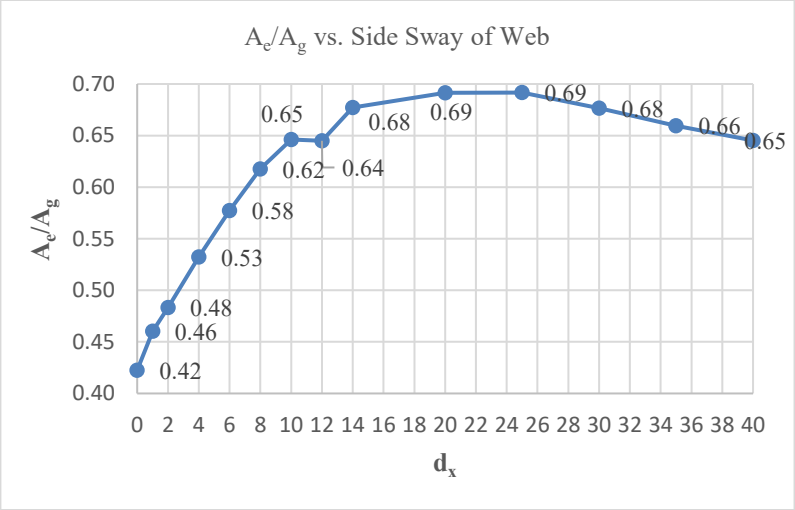

Fig. 7 The effect of d_x on effective area ratio

2.2. Effect of d_x on Euler Buckling Stress (F_n)

In Fig. 8, the effect of d_x on Euler buckling stress is illustrated. As it is shown, the minimum Euler buckling stress is 31.56 ksi (217.63 Mpa) at d_x=0 and the maximum one is 33.36 ksi (230 Mpa) at d_x=1.5748”(40 mm). The difference between the minimum and maximum is about 1.74 ksi (12 Mpa). So d_x is not an influential feature on Euler buckling stress. However the trend of the curve variations is investigated. As depicted in Fig. 8, the Euler buckling stress is growing in the region of $0 \leq d_x < 0.5512$”(14 mm); the governing buckling mode in this region is flexural-torsional buckling (Eq. 1-3). In order to investigate the influential torsional section properties on flexural-torsional buckling, the Eq. 1 is under attention. Next, the effect of d_x on C_ω and r_0 is evaluated and results are depicted in Fig. 9 and Fig. 10. The square of r_0 is the dominant parameter on Euler buckling stress as it is evident from comparison of Fig. 8 and Fig. 9 that the slope steepness of the curve in Fig. 8 in the region $0 \leq d_x < 0.5512$”(14 mm) is compatible with slope trend of the curve in Fig. 9.

$$\sigma_t = \frac{1}{A{r_0}^2}.(GJ + \frac{\pi^2.E.C_w}{(k_t.L_t)^2}) \qquad [1]$$

$$\sigma_{ex} = \frac{\pi^2.E}{(\frac{k_y.L_x}{r_x})^2} \quad [2]$$

$$F_{et} = \frac{1}{2\beta}.\left[(\sigma_{ex} + \sigma_t) - \sqrt{(\sigma_{ex} + \sigma_t)^2 - 4.\beta.\sigma_{ex}.\sigma_t}\right] \quad [3]$$

$$\sigma_{ey} = \frac{\pi^2.E}{(\frac{k_y.L_y}{r_y})^2} \quad [4]$$

In the region of 0.5512”(14 mm)≤d_x≤1.3779”(35 mm), flexural buckling about weak axis (Y-axis) is the governing buckling mode (Eq. 4), so the key parameter on the value of Euler buckling stress is r_y. As depicted in Fig. 11, in the region of 0.5512”(14 mm)≤d_x≤0.7874”(20 mm), increase in d_x makes reduction in r_y, so the Euler buckling stress has a decreasing trend in this region. In the region of 0.7874”(20 mm)≤d_x≤1.3779”(35 mm), as the value of r_y increases, the Euler buckling stress starts augmenting. At the d_x=1.5748”(40 mm), again, the buckling mode will change to flexural-torsional buckling, but not considerable change in value of this stress is evident rather than the value at d_x=1.3779”(35 mm).

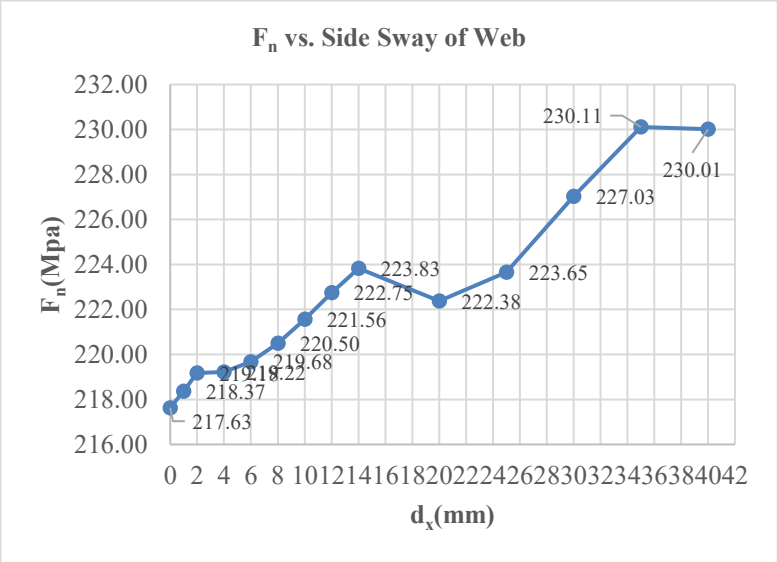

Fig. 8 The effect of d_x on Euler buckling stress

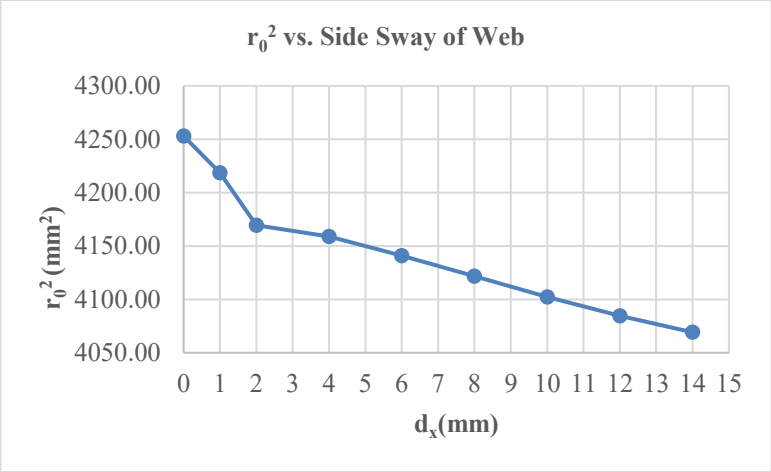

Fig. 9 The effect of d_x on square of Polar radius of gyration

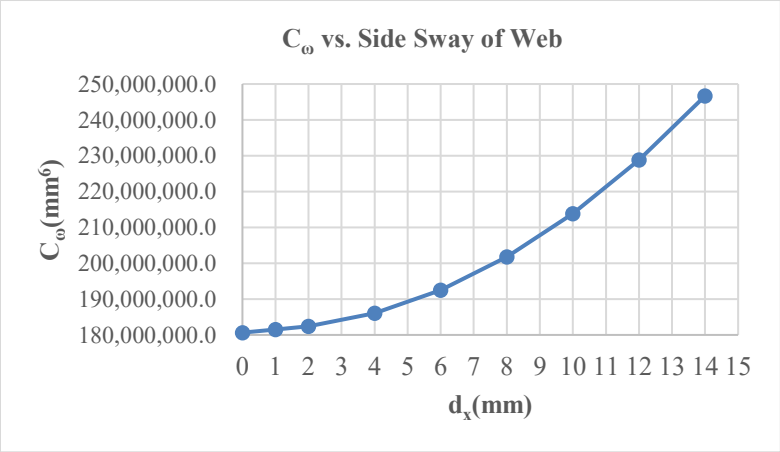

Fig. 10 The effect of d_x on square of Polar radius of gyration

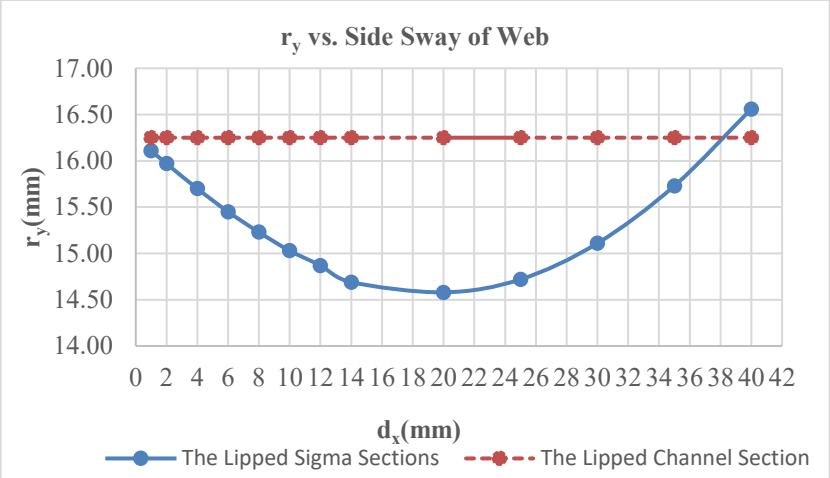

Fig. 11 The effect of d_x on Radius of gyration respect toY centroidal principal axis

2.3. Effect of d_x on Euler-Local Buckling Strength (P_n)

Nominal Euler-local strength of the **lipped Σ section/lipped C section**	$P_{n\Sigma}/P_{nC}$

After the investigation of d_x variations on effective area ratio and Euler buckling stress, it is possible to discuss about the Euler-local buckling strength. As illustrated in Fig. 12, in the region of $0 \leq d_x \leq 0.5512$"(14 mm), the $P_{n\Sigma}/P_{nC}$ ratio is increasing with a steep slope. After d_x=0.5512"(14 mm) the slope of the curve starts decreasing.

From the optimum design point of view of a cross section, in addition to having stronger section by stiffening the web, it is important to know that how much increase in cross-section area makes section stronger. Therefore, the trend of increase in cross sectional area vs. d_x is depicted in Fig. 13. Comparing the Fig. 12 with Fig. 13, at d_x=0.3937"(14 mm), the $P_{n\Sigma}/P_{nC}$ ratio is 1.54 and Increase in cross-sectional area is 5.24%, i.e. 54% increase in the Euler-local buckling strength of the lipped Σ section rather than the equivalent lipped C section for 5.24% augmentation in the cross-sectional area. Also, at d_x=0.7874"(20 mm), the $P_{n\Sigma}/P_{nC}$ ratio is 1.88 and Increase in cross-sectional area is 12.70%, i.e. 88%

increase in the Euler-local buckling strength of the lipped Σ section rather than the equivalent lipped C section for 12.70% augmentation in the cross-sectional area. Therefore, comparing above results demonstrate that 5.24% increase of the cross-sectional area due to the web stiffening and giving 54% increment in the strength of the cross section may be a more economical choice rather than 12.7% increase of the cross-sectional area and giving 88% increment in the strength of the cross section.

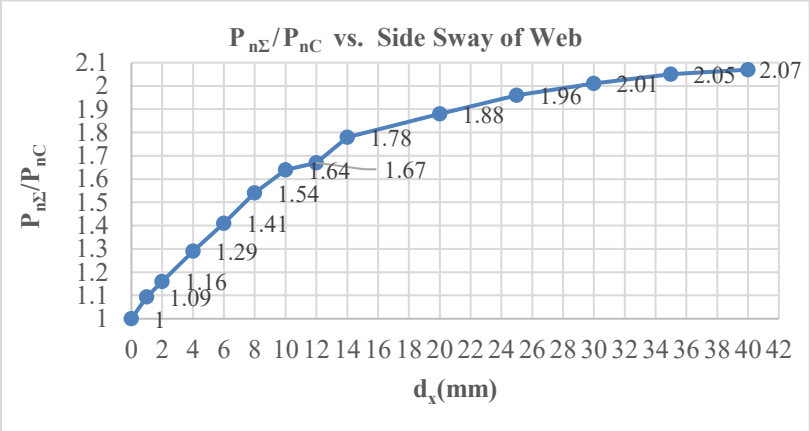

Fig. 12 The effect of d_x on $P_{n\Sigma}/P_{nC}$

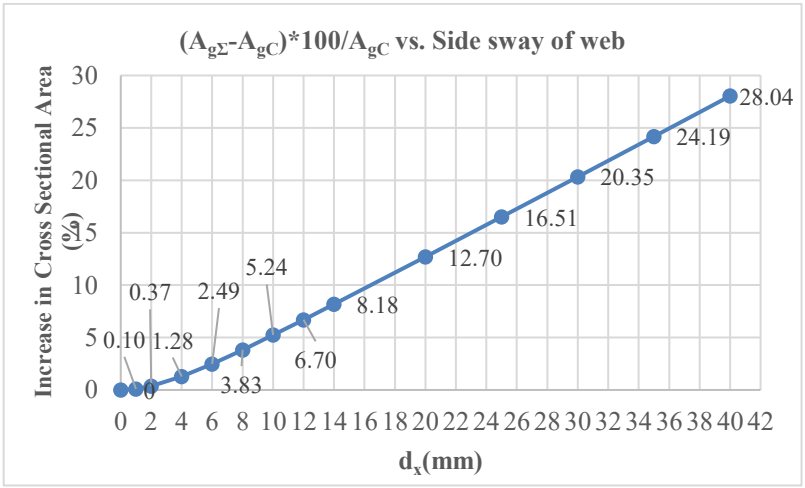

Fig. 13 The effect of d_x on Increase in cross sectional area

2.4. Effect of d_x on Distortional Buckling Stress (F_{nd})

The distortional buckling stress for the lipped C section may be easily computed by the conventional method of the specification (*AISI S100-16, North American Specification for the Design of Cold-Formed Steel Structural Members, Commentary* 2016), but for the lipped Σ section it is not possible to calculate this buckling stress by conventional method. Therefore, to calculate the distortional buckling stress of the lipped Σ sections, the direct strength method (DSM) (*AISI S100-16, North American Specification for the Design of Cold-Formed Steel Structural Members* 2016, *AISI S100-16, North American Specification for the Design of Cold-Formed Steel Structural Members, Commentary*, *Direct Strength Method (DSM) Design Guide Committee on Specifications for the Design of Cold-Formed Steel Structural Members* 2006; Schafer and Peköz 1998) is utilized. As illustrated in Fig. 14, the minimum Euler buckling stress is 116.64 Mpa at d_x=0.03937"(1 mm) and the maximum one is 218.07 Mpa at d_x=1.3779"(35 mm). The difference between the minimum and maximum is about 101Mpa. So d_x is a key feature on distortional buckling stress. In the region of 0≤dx≤1.3779"(35 mm), except for d_x=0.03937"(1 mm), the increase in the d_x, augments the distortional buckling stress.

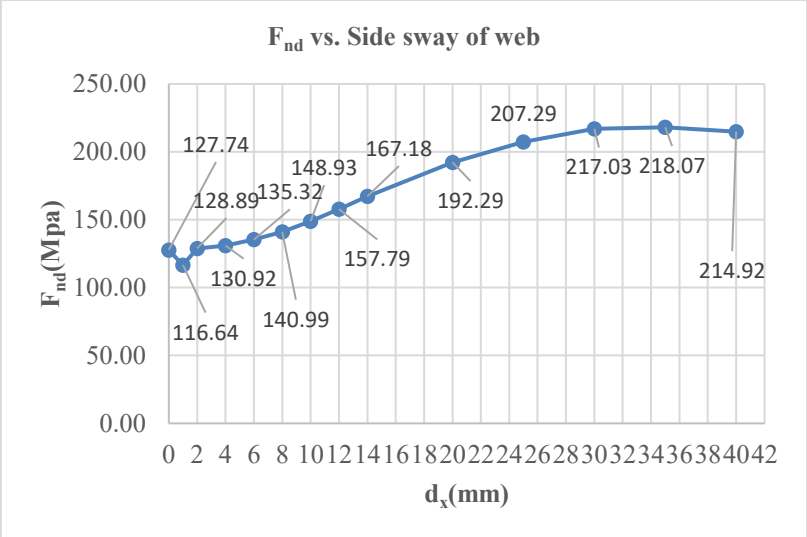

Fig. 14 The effect of d_x on Increase in distortional buckling stress

2.5. Effect of d_x on Distortional Buckling Strength

Nominal distortional strength of the **lipped Σ section/lipped C section**	$P_{nd\Sigma}/P_{ndC}$

In Fig. 15, the effect of d_x variation on $P_{nd\Sigma}/P_{ndC}$ ratio is depicted. In the region of $0 \leq dx \leq 1.5748$"(40 mm), except for $d_x=0.03937$"(1 mm), the trend of the $P_{nd\Sigma}/P_{ndC}$ ratio variations is always increasing.

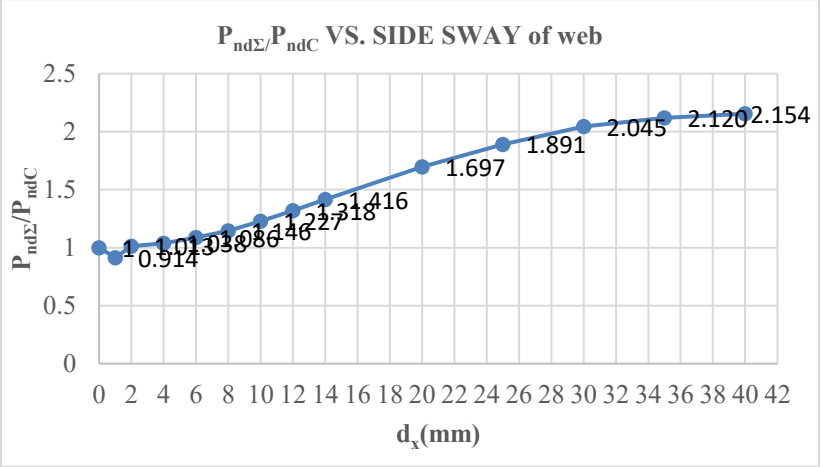

Fig. 15 The effect of d_x on $P_{nd\Sigma}/P_{ndC}$

3. Comparison of Euler-local buckling strength and Distortional buckling strength

In Fig. 16, the Euler-local buckling strength is compared with distortional buckling strength. For all values of the d_x, except for the values in the region of 0.15748"(4 mm)$<d_x<0.5512$"(14 mm), distortional buckling strength is the higher value. At $d_x=0.15748$"(4 mm), $d_x=0.4724$"(12 mm) and $d_x=0.5512$"(14 mm), these 2 strengths are almost equal and their values are about 4.592 kips (2.05 ton_f), 5.824 kips (2.60ton_f) and 6.272 kips (2.80ton_f), respectively. As the interaction of local-distortional and Euler buckling is probable at aforementioned points, it is recommended to avoid these side sways in the design of the cross section.

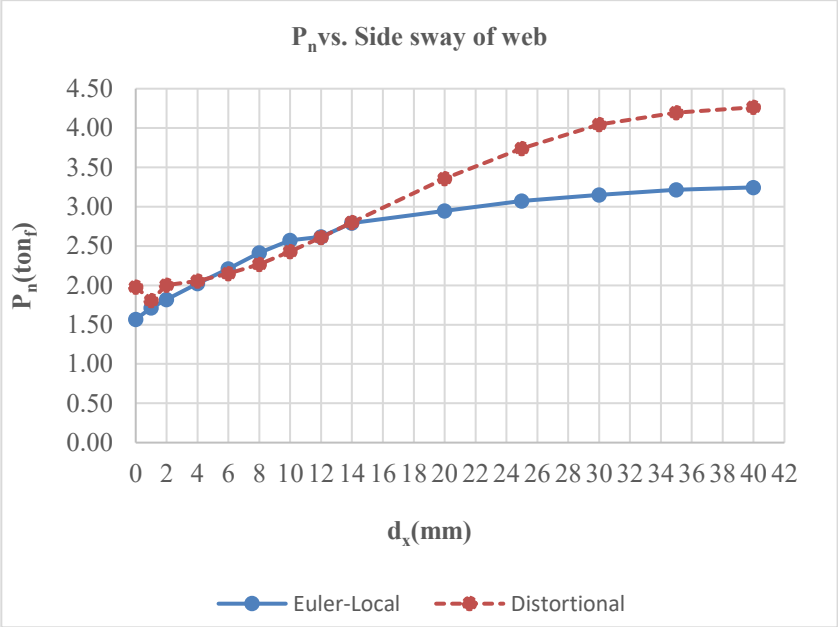

Fig. 16 Comparison of Euler-local and distortional buckling strengths

Conclusion

In this research, the effect of web stiffening of cold-formed steel thin-walled lipped sigma sections in compression members is investigated. d_x, the amount of inward side sway of the web, or the horizontal projection of web stiffeners' length, is selected as the main variable. The effect of d_x variations is evaluated on buckling behavior and buckling strengths of the lipped Σ section and the following results are obtained.

1-In the region of $0 \leq d_x < 0.5512$"(14 mm), the inclined elements of the web act like stiffeners and change the buckled mode shape of the section from local buckling into distortional buckling, but for $d_x \geq 0.5512$"(14 mm) the inclined elements of the web act like independent elements and change the buckled mode shape of the section from distortional buckling into local buckling of sub-elements of the web and other elements of the section.

2- As the preceding result was obtained, in the calculation of effective width, for $d_x \geq 0.5512$”(14 mm), the inclined elements were considered as independent elements rather than stiffening elements. Therefore, modified effective width was calculated for $d_x \geq 0.5512$”(14 mm).

3-As d_x increases, the effective area ratio (A_e/Ag) increments. The maximum of this ratio is 0.69 at d_x=0.7874”, 0.9842”, (20, 25 mm). However the optimum effective area ratio with the consideration of less cross-sectional area may be 0.65 at d_x=0.39370”(10 mm).

4-d_x variations do not have considerable impact on the Euler buckling stress. As presented, the difference between the minimum and maximum distortional buckling stresses is about 1.74 ksi (12 Mpa).

5-d_x variations have considerable effect on the distortional buckling stress. As demonstrated, the difference between the minimum and maximum distortional buckling stresses is about 14.79ksi (102 Mpa).

6- As d_x increments, in the region of $0 \leq d_x < 0.5512$”(14 mm) the Euler-local buckling strength increases with a steep slope and after that region with a mild slope, but the distortional buckling strength , in the region of $0 \leq d_x < 0.5512$”(14 mm augments with an incremental slope and after that region with an decreasing slope.

7- From optimum design point of view, a lipped Σ section is one that have the closest nominal Euler-local and distortional buckling strengths, but it should be considered to avoid nearly equal values of these buckling strengths because of the probable local-distortional and Euler buckling interaction. Therefore, the best optimum region is 0.15748”(4 mm)$< d_x <$0.47244”(12 mm) and the best d_x is equal to 0.39370”(10 mm).

Appendix.-References

AISI S100-16, North American Specification for the Design of Cold-Formed Steel Structural Members. (2016). .

AISI S100-16, North American Specification for the Design of Cold-Formed Steel Structural Members, Commentary. (2016). .

CUFSM. (2006). “CUFSM v4.05.”

Direct Strength Method (DSM) Design Guide Committee on Specifications for the Design of Cold-Formed Steel Structural Members. (2006). .

Schafer, B. W. (2011). “Cold-formed steel structures around the world.” Steel Construction.

Schafer, B. W., and Ádány, S. (2006). “Buckling analysis of cold-formed steel members using CUFSM: conventional and constrained finite strip methods.” 18th International Specialty Conference on Cold-Formed Steel Structures October 26-27, Orlando, Florida, 17–31.

Schafer, B. W., and Peköz, T. (1998). “Direct strength prediction of cold-formed steel members using numerical elastic buckling solutions.” Fourteenth International Specialty Conference on Cold-Formed Steel Structures: Recent Research and Developments in Cold-Formed Steel Design and Construction, 69–76.

Wang, C., Zhang, Z., Zhao, D., and Liu, Q. (2016). “Compression tests and numerical analysis of web-stiffened channels with complex edge stiffeners.” Journal of Constructional Steel Research, Elsevier Ltd, 116, 29–39.

Yang, D., and Hancock, G. J. (2004). “Compression Tests of High Strength Steel Channel Columns with Interaction between Local and Distortional Buckling.” (December), 1954–1963.

Yap, D. C. Y., and Hancock, G. J. (2008). School of Civil Engineering Sydney NSW 2006 Centre for Advanced Structural Engineering Experimental Study of High Strength Cold-Formed Stiffened Web Steel Sections Experimental Study of High Strength Cold-Formed.

Yap, D. C. Y., and Hancock, G. J. (2011). “Experimental Study of High-Strength Cold-Formed Stiffened-Web C-Sections in Compression.” Journal of Structural Engineering, 137(2), 162–172.

Appendix.-Notations

Dimensions:

t : Base steel thickness
W: Back to back width of the web
B: Back to back width of the flange
D: Distance from Back of the flange to the end of the lip
r' : Inner radius of the bent (=2t)
d_x : Horizontal projection of the web stiffeners' length (Side sway of web)
d_y : Vertical projection of the web stiffeners' length
$\bar{a}$: Back to back width of the web minus a thickness
$\bar{a}_1$: Distance from the middle axis of the above flange to the beginning of the web stiffener
$\bar{a}_2$: Middle width of the web between two web stiffeners
$\bar{a}_3$: Distance from the middle axis of the below flange to the beginning of the web stiffener
$\bar{b}$: Distance from middle axis of the web to middle axis of the lip
$\bar{c}$: Distance from middle axis of the flange to end of the lip

General section properties:

A : Full unreduced Cross sectional area of member
A_e : Effective Cross sectional area ofmember
I_x, I_y : Moment of Inertia of full unreduced section respect to X, Y principal centroidal axis
r_x, r_y :Radius of gyration respect to the X, Y principal centroidal axis
K_x, K_y :Effective length factors for *buckling* about x, y-axis
L_x , L_y : Unbraced lengths for elastic Euler buckling about x-axis and y-axis

Torsional and warping properties of the cross section

J : Saint-Venant torsion constant
C_ω : Torsional warping constant
$\bar{x}$: Distance from shear plane to centroid of cross-section
m : Distance from shear plane to shear center in principal x-axis direction
X_0 : Distance from centroid to shear center in principal x-axis direction
r_o : Polar radius of gyration of cross-section about shear center
$\beta=1-(x_0/r_0)^2$
K_t Effective length factor for torsion
L_t : Unbraced length for torsional buckling about longitudinal axis

Euler Buckling Stresses

σ_{ex} :Elastic Euler buckling stress about x-axis
σ_{ey} :Elastic Euler buckling stress about y-axis
σ_t :Torsional buckling stress
F_{et} :Flexural-torsional buckling stress
p_{cr}/p_y : Load factor (Ratio of the critical buckling load to the yield load)